

Influence of depth habitat on carbonate $\delta^{18}\text{O}$. In general, $\delta^{18}\text{O}$ records are influenced by a combination of local temperature and salinity, and global ice volume variations (Chappell and Shackleton, 1986; Maslin et al., 1995; Rohling, 2000; Shackleton, 1974, 1987). If we assume constant ice volume for a snapshot in time, the foraminifera $\delta^{18}\text{O}$ signal mostly reflects the temperature of the water mass where it calcified (Schmidt and Mulitza, 2002; Mulitza et al., 2003; Schiebel and Hemleben, 2005). Therefore, $\delta^{18}\text{O}$ can be used to infer the depth habitat of different foraminifera species, with higher $\delta^{18}\text{O}$ indicating deeper and colder water masses (e.g., Mulitza et al. (1997), Rashid and Boyle (2007) and references therein). Accordingly, lower $\delta^{18}\text{O}$ of *T. sacculifer* and *G. ruber* relative to *G. truncatulinoides*, *G. bulloides*, and *G. siphonifera* can be explained by their shallower depth habitats. Assuming constant $\delta^{18}\text{O}$ of seawater, we convert $\delta^{18}\text{O}$ of our most recent foraminiferal calcite data (2-3 Holocene samples) to temperature of calcification using an online tool (Gaskell and Hull (2022), version 1.2) and compare it with the modern temperature depth profile for a South Atlantic station (30.5°S, 34.5°W) close to our site (World Ocean Atlas, WOA18,) (Fig. S6). Accordingly, *T. sacculifer* and *G. ruber* calcify in ~19°C waters at ca. 100 m water depth. *Globigerinella siphonifera* calcify at ~16°C (i.e., ~200 m $\delta^{18}\text{O}$ depth) and *G. truncatulinoides* and *G. bulloides* have the lowest calcification temperature of ~11°C (i.e., ~ 400-500 m $\delta^{18}\text{O}$ depth). Previous studies in the South Atlantic subtropical gyre suggest a similar upper mixed layer depth habitat for *T. sacculifer* and *G. ruber* (Lessa et al., 2020). In contrast, both *G. siphonifera* Types I and II typically present maximum abundance between 50 m and 100 m water depth spanning the upper to lower deep chlorophyll maximum in the tropics and subtropical ocean (Rebotim et al., 2017; Schiebel and Hemleben, 2017; Schiebel, 2002), which is shallower than inferred from $\delta^{18}\text{O}$ -derived calcification temperatures and a local temperature profile. The same type of discrepancy exists for *G. bulloides*, which typically dwells at surface to thermocline depths. This supports a non-local origin for these two species; i.e., a substantial fraction of these may have calcified in shallower waters of a cooler environment (see Section 4.4.3 on lateral transport).

Influence of seasonality on carbonate $\delta^{18}\text{O}$ and $\delta^{13}\text{C}$. In addition to depth habitat, the $\delta^{18}\text{O}$ -derived temperature signal preserved in deep-sea sediments depends on seasonal changes in ocean temperatures and shell production and reflects an integrated signal across its seasonal range with a bias towards the season of highest production (Deuser and Ross, 1989; Tedesco et al., 2007; Thunell and Sautter, 1992). Based on foraminifera species counts in the North Atlantic, *T. sacculifer* records highest abundances in summer and fall. *Globigerinoides ruber* are associated with thermal maxima in the North Atlantic in summer. *Globigerinella siphonifera* appear to have a bimodal abundance distribution with peaks in spring and fall and *G. truncatulinoides* are an indicator of late winter/early spring conditions. The main production of *G. bulloides* occurs in spring (Salmon et al., 2015; Tolderlund and Bé, 1971). We expect similar seasonality of production at Site 516.

Biological and thermodynamic processes in the surface water and underlying water column, such as primary production, respiration, and air-sea gas exchange can potentially cause seasonal variability in dissolved inorganic carbon (DIC) concentration and the $\delta^{13}\text{C}_{\text{DIC}}$ (Charles et al., 1993). However, shallow surface seawater data from the South Atlantic show only little variation between summer and winter. Throughout the year, surface $\delta^{13}\text{C}_{\text{DIC}}$ remains between 1.5 ‰ and 1.75 ‰ (Gruber et al., 1999). Therefore, we expect little or no effect of seasonality on interspecies- $\delta^{13}\text{C}$ at Site 516.

Results for nitrate $\delta^{15}\text{N}$ analyses. The vertical profiles of nitrate concentration ($[\text{NO}_3^-]$) from southern CLIMODE stations (<37.5°N) show a distribution that is characteristic of the subtropical North Atlantic (Knapp et al., 2005). $[\text{NO}_3^-]$ decreases upward from an average of 24 μM near the base of the thermocline (800–1000 m) to 0–0.5 μM at the near-surface, with a depth zone of relatively constant $[\text{NO}_3^-]$ between 200 and 500 m that reflects 18° Water (Fig. S4). A strong latitudinal variation in $[\text{NO}_3^-]$ was observed in the typical upper thermocline depth zone (800–1000 m), increasing from 3–5 μM at the southernmost station to ~25 μM at northernmost station (38.6°N). Surface samples from the northernmost station have an average $[\text{NO}_3^-]$ of 3.2 μM which is comparable to $[\text{NO}_3^-]$ in the upper thermocline water at the BATS site.

The vertical structure of $\delta^{15}\text{N}$ in the southernmost CLIMODE stations is similar to that observed in the lower latitude Sargasso Sea (Knapp et al., 2005; Fawcett et al., 2015). The $\delta^{15}\text{N}$ starts to decrease from an average of $\sim 5.3\text{‰}$ at ~ 800 m depth and reaches its minimum of $\sim 2.0\text{‰}$ at ~ 200 m. Along the south to north CLIMODE transect, the upward decline in $\delta^{15}\text{N}$ becomes smaller, becoming absent in profiles from $>38.0^\circ\text{N}$. Every $\delta^{15}\text{N}$ profile shows a sharp rise toward the surface above ~ 200 m depth, which is the effect of nitrate assimilation approaching completion in the euphotic zone (Fawcett et al., 2015).

Water masses originating from the Southern Ocean exhibit higher $[\text{NO}_3^-]$. The vertical profiles of $[\text{NO}_3^-]$ at the South Atlantic stations along the A13.5 transect reveal the highest $[\text{NO}_3^-]$ in the lower thermocline (~ 1200 m; characterized by Antarctic Intermediate Water, AAIW) and at the bottom depths (Antarctic Bottom Water, AABW). North Atlantic Deep Water (NADW), occupying the depths between AAIW and AABW, shows $[\text{NO}_3^-]$ around $25\text{ }\mu\text{M}$. $[\text{NO}_3^-]$ decreases upward, from $\sim 33\text{ }\mu\text{M}$ in the AAIW to near zero in stations north of 37°S , while the surface waters of the stations between 42°S and 41°S bear less than $7.6\text{ }\mu\text{M}$ of nitrate.

In terms of nitrate $\delta^{15}\text{N}$, the deep water in the South Atlantic stations shows values around 4.8 ‰ near the bottom of the profile, close to the mean nitrate $\delta^{15}\text{N}$ of NADW (Marconi et al., 2015). The nitrate $\delta^{15}\text{N}$ gradually increases upwards. From an average of $\sim 5.2\text{ ‰}$ at ~ 1500 m depth, $\delta^{15}\text{N}$ rises to $\sim 6.6\text{ ‰}$ at 200 m. As in the North Atlantic, nitrate $\delta^{15}\text{N}$ increases sharply toward the surface due to assimilation by phytoplankton (Fawcett et al., 2015).

Supplementary Tables:

Table S1. Slope, R², r-value (Pearson correlation coefficient) and p-values for size-specific $\delta^{18}\text{O}$ and $\delta^{13}\text{C}$ measurements on different foraminifera species in Site 516.

	Glacial - 27 ka				Interglacial - 129 ka				combined			
	slope	R ²	r-value	p-value	slope	R ²	r-value	p-value	slope	R ²	r-value	p-value
size-specific $\delta^{18}\text{O}$												
<i>G. ruber albus</i>	-0.0010	0.46	-0.68	0.32	-0.0007	0.22	-0.47	0.53	-0.0009	0.97	-0.98	0.02
<i>G. ruber ruber</i>	-0.0015	0.88	-0.93	0.07	0.0013	0.59	0.77	0.23	-0.0001	0.09	-0.31	0.69
<i>T. sacculifer</i>	-0.0015	0.62	-0.78	0.22	-0.0012	0.78	-0.88	0.12	-0.0014	0.71	-0.84	0.16
<i>G. truncatulinoides</i>	0.0009	0.13	0.36	0.64	0.0002	0.01	0.07	0.93	0.0005	0.06	0.24	0.76
<i>G. siphonifera</i>	0.0004	0.30	0.51	0.49	0.0004	0.62	0.77	0.23	0.0004	0.50	0.73	0.27
<i>G. bulloides</i>	0.0073	n/a	n/a	n/a	0.0017	n/a	n/a	n/a	0.0045	n/a	n/a	n/a
size-specific $\delta^{13}\text{C}$												
<i>G. ruber albus</i>	0.0050	0.95	0.98	0.02	0.0018	0.25	0.93	0.07	0.0034	0.76	0.87	0.13
<i>G. ruber ruber</i>	0.0035	0.95	0.97	0.03	0.0050	0.86	0.93	0.07	0.0043	0.91	0.95	0.05
<i>T. sacculifer</i>	0.0035	0.80	0.90	0.10	0.0071	0.93	0.96	0.04	0.0053	0.91	0.96	0.04
<i>G. truncatulinoides</i>	0.0043	0.83	0.91	0.09	0.0038	0.46	0.68	0.32	0.0040	0.75	0.87	0.13
<i>G. siphonifera</i>	0.0013	0.36	0.60	0.40	0.0024	0.75	0.86	0.14	0.0018	0.60	0.77	0.23
<i>G. bulloides</i>	0.0028	n/a	n/a	n/a	0.0036	n/a	n/a	n/a	0.0032	n/a	n/a	n/a

Table S2. Core top FB- $\delta^{15}\text{N}$ compilation used for Figure 5 and 6.

Location/ Core Site	Core ID	latitude	longitude	foraminifera species	reference
Barbuda-Antiqua	Barbuda-Antiqua	17.50	-61.00	<i>G. ruber albus</i> , <i>T. sacculifer</i> , <i>O. universa</i>	Ren et al. (2012)
BATS	BATS	31.73	-64.08	<i>G. ruber albus</i> , <i>O. universa</i> , <i>G. menardii</i> , <i>N. dutertrei</i> , <i>G. hirsuta</i> , <i>G. inflata</i> , <i>G. truncatulinoides</i>	Smart et al. (2018)
Cariaco Basin	Cariaco Basin	10.70	-64.70	<i>G. ruber albus</i> , <i>T. sacculifer</i> , <i>O. universa</i> , <i>G. menardii</i> , <i>G. dutertrei</i> , <i>G. siphonifera</i>	Ren et al. (2012)
Cariaco Basin	Cariaco Basin	10.50	-64.70	<i>G. ruber albus</i> , <i>T. sacculifer</i> , <i>O. universa</i>	Schiebel et al. (2018)
DSDP 516	DSDP 516	-30.28	-35.29	<i>G. ruber albus</i>, <i>G. ruber ruber</i>, <i>T. sacculifer</i>, <i>G. siphonifera</i>, <i>G. truncatulinoides</i>, <i>G. bulloides</i>	this study
Eq. Atlantic 1	V25-75TW	8.58	-53.17	<i>G. ruber albus</i> , <i>T. sacculifer</i> , <i>O. universa</i>	Schiebel et al. (2018)
Eq. Atlantic 2	Bill-22	7.00	-49.50	<i>G. ruber albus</i> , <i>T. sacculifer</i> , <i>O. universa</i>	Schiebel et al. (2018)
Eq. Atlantic 3	RC13-184TW	3.87	-43.30	<i>G. ruber albus</i> , <i>T. sacculifer</i> , <i>O. universa</i>	Schiebel et al. (2018)
Eq. Atlantic 4	V25-60TW	3.28	-34.83	<i>G. ruber albus</i> , <i>T. sacculifer</i> , <i>O. universa</i>	Schiebel et al. (2018)
Eq. Atlantic 5	V25-59TW	1.37	-33.48	<i>G. ruber albus</i> , <i>T. sacculifer</i> , <i>O. universa</i>	Schiebel et al. (2018)
Eq. Atlantic 6	V25-56TW	-3.55	-34.23	<i>G. ruber albus</i> , <i>T. sacculifer</i> , <i>O. universa</i>	Schiebel et al. (2018)
Eq. Atlantic 7	V22-38TW	-9.55	-34.25	<i>G. ruber albus</i> , <i>T. sacculifer</i> , <i>O. universa</i>	Schiebel et al. (2018)
Eq. Atlantic 8	RC13-189TW	1.87	-30.00	<i>G. ruber albus</i> , <i>T. sacculifer</i> , <i>O. universa</i>	Schiebel et al. (2018)
Eq. Atlantic 9	V30-36TW	5.35	-27.32	<i>G. ruber albus</i> , <i>T. sacculifer</i> , <i>O. universa</i>	Schiebel et al. (2018)
Eq. Atlantic 10	V30-40TW	-0.20	-23.15	<i>G. ruber albus</i> , <i>T. sacculifer</i> , <i>O. universa</i>	Schiebel et al. (2018)
Eq. Atlantic 11	V30-41TW	0.22	-23.07	<i>G. ruber albus</i> , <i>T. sacculifer</i> , <i>O. universa</i>	Schiebel et al. (2018)
Eq. Atlantic 12	V22-182TW	-0.55	-17.27	<i>G. ruber albus</i> , <i>T. sacculifer</i> , <i>O. universa</i>	Schiebel et al. (2018)
Eq. Pacific a	14MC: 0-8	-0.22	204.04	<i>G. ruber albus</i> , <i>T. sacculifer</i> , <i>G. tumida</i>	Costa et al. (2016)
Eq. Pacific b	21MC: 0-8	1.27	202.74	<i>G. ruber albus</i> , <i>T. sacculifer</i> , <i>G. tumida</i>	Costa et al. (2016)
Eq. Pacific c	26MC: 0-8	2.46	200.61	<i>G. ruber albus</i> , <i>T. sacculifer</i> , <i>G. tumida</i>	Costa et al. (2016)
Eq. Pacific d	29MC: 0-8	2.97	200.80	<i>G. ruber albus</i> , <i>T. sacculifer</i> , <i>G. tumida</i>	Costa et al. (2016)
Eq. Pacific e	33MC: 0-8	5.2	199.57	<i>G. ruber albus</i> , <i>T. sacculifer</i> , <i>G. tumida</i>	Costa et al. (2016)
Eq. Pacific f	39MC: 0-8	6.83	198.96	<i>G. ruber albus</i> , <i>T. sacculifer</i> , <i>G. tumida</i>	Costa et al. (2016)
Great Bahama Banks	Great Bahama Banks	24.30	-79.20	<i>G. ruber albus</i> , <i>T. sacculifer</i> , <i>O. universa</i> , <i>G. menardii</i> , <i>G. dutertrei</i> , <i>G. siphonifera</i>	Ren et al. (2012)
Hawaii	Hawaii	20.80	-157.30	<i>G. ruber albus</i> , <i>T. sacculifer</i>	Ren et al. (2012)
Indonesia	Indonesia	-6.8	117.00	<i>G. ruber albus</i> , <i>T. sacculifer</i> , <i>O. universa</i> , <i>G. menardii</i> , <i>G. dutertrei</i> , <i>G. siphonifera</i>	Ren et al. (2012)
New Zealand	New Zealand	-36.4	176.70	<i>G. ruber albus</i> , <i>O. universa</i> , <i>G. siphonifera</i>	Ren et al. (2012)
ODP 1090	ODP 1090	-42.91	8.90	<i>O. universa</i> , <i>G. bulloides</i>	Martínez-García et al. (2014)
ODP 662	ODP 662	-1.38	-11.78	<i>T. sacculifer</i> , <i>N. dutertrei</i>	Auderset et al. (2024)
San Pedro Basin	San Pedro Basin	33.50	-118.00	<i>O. universa</i> , <i>N. dutertrei</i>	Ren et al. (2012)
South China Sea	South China Sea	12.70	119.50	<i>G. ruber albus</i> , <i>T. sacculifer</i> , <i>O. universa</i> , <i>G. menardii</i> , <i>G. dutertrei</i> , <i>G. siphonifera</i>	Ren et al. (2012)

Supplementary Figures:

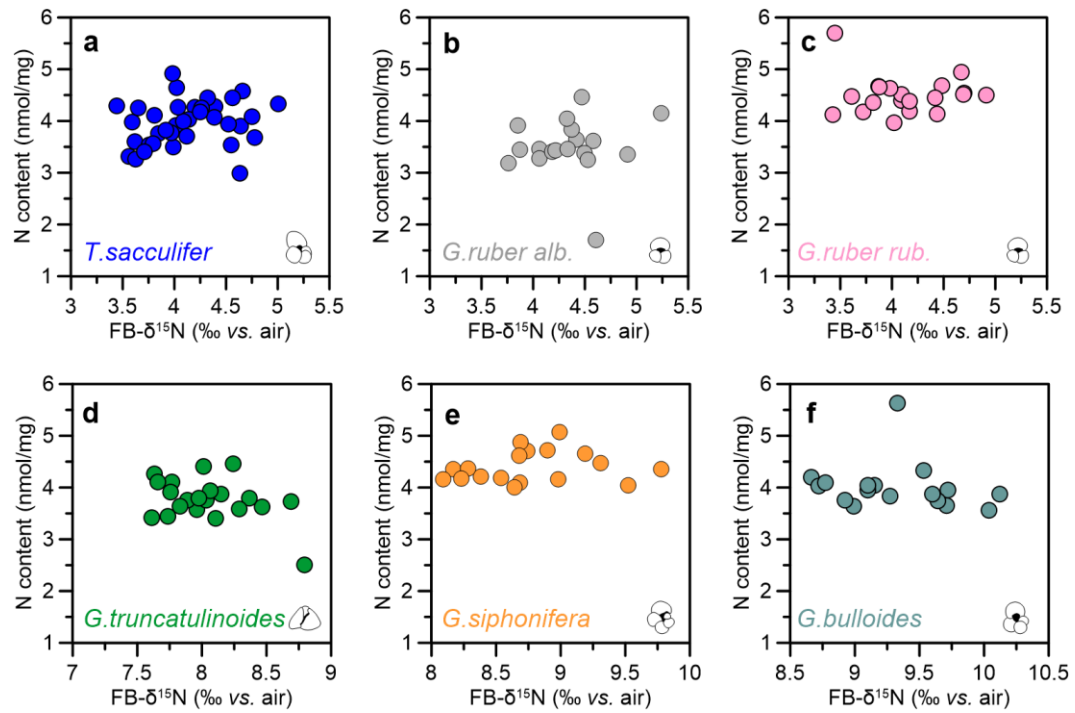


Figure S1. No correlation between N content and FB- $\delta^{15}\text{N}$ for studied foraminiferal species (a-f) indicating no effect of diagenesis on FB- $\delta^{15}\text{N}$ signal.

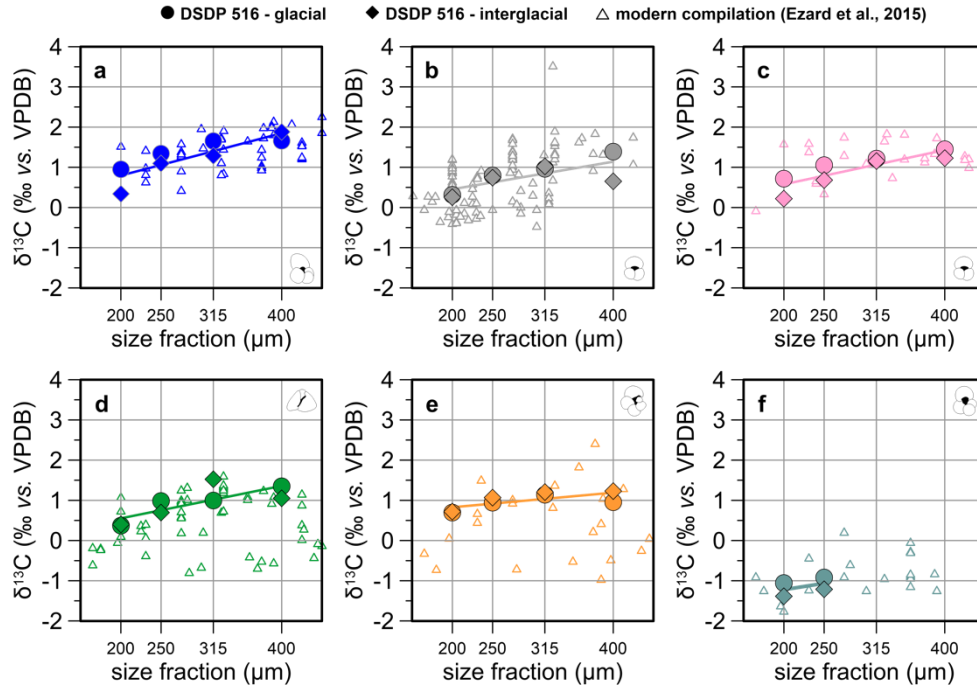


Figure S2. Size-specific $\delta^{13}\text{C}$ with linear fits. Carbon isotopes measured on calcite of (a) *T. sacculifer*, (b) *G. ruber albus* (c) *G. ruber ruber*, (d) *G. truncatulinoides*, (e) *G. siphonifera*, and (f) *G. bulloides* in DSDP 516 sediment samples from two time slices: glacial (Last Glacial Maximum, 27 ka, circles) and-interglacial (Marine Isotope Stage 5, 127 ka, diamonds). Data in comparison with size-specific carbon isotope compilation by Ezard et al. (2015) (triangles). Linear fit through average of size-specific $\delta^{13}\text{C}$ for both time slices in DSDP 516.

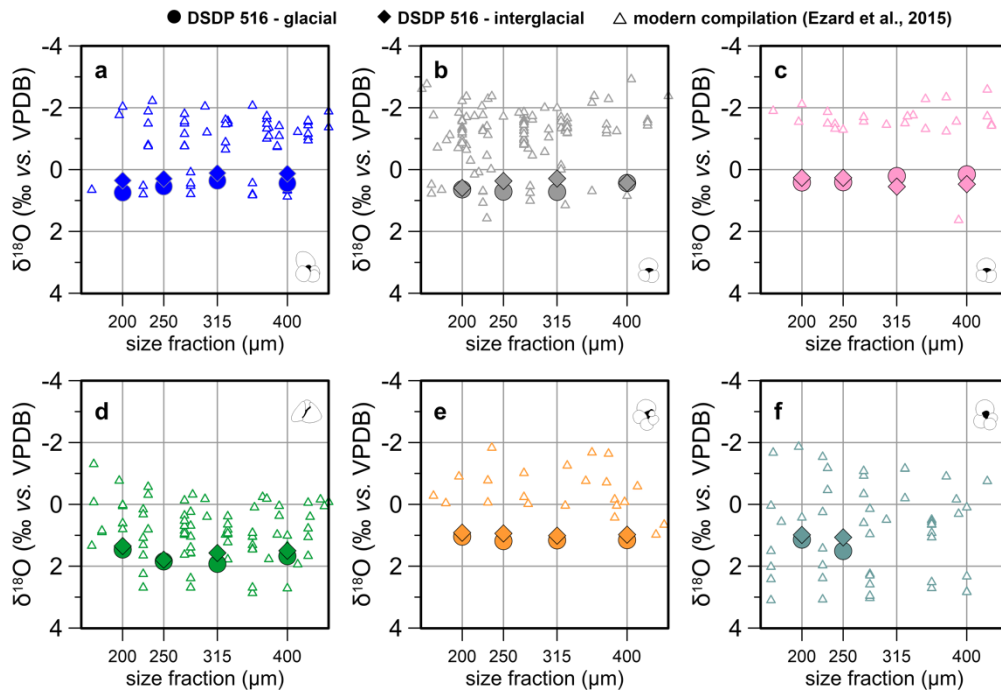


Figure S3. Size-specific $\delta^{18}\text{O}$. Oxygen isotopes measured on calcite of (a) *T. sacculifer*, (b) *G. ruber albus* (c) *G. ruber ruber*, (d) *G. truncatulinoides*, (e) *G. siphonifera*, and (f) *G. bulloides* in DSDP 516 sediment samples from two time slices: glacial (Last Glacial Maximum, 27 ka, circles) and-interglacial (Marine Isotope Stage 5, 127 ka, diamonds). Data in comparison with size-specific oxygen isotope compilation by Ezard et al. (2015) (triangles).

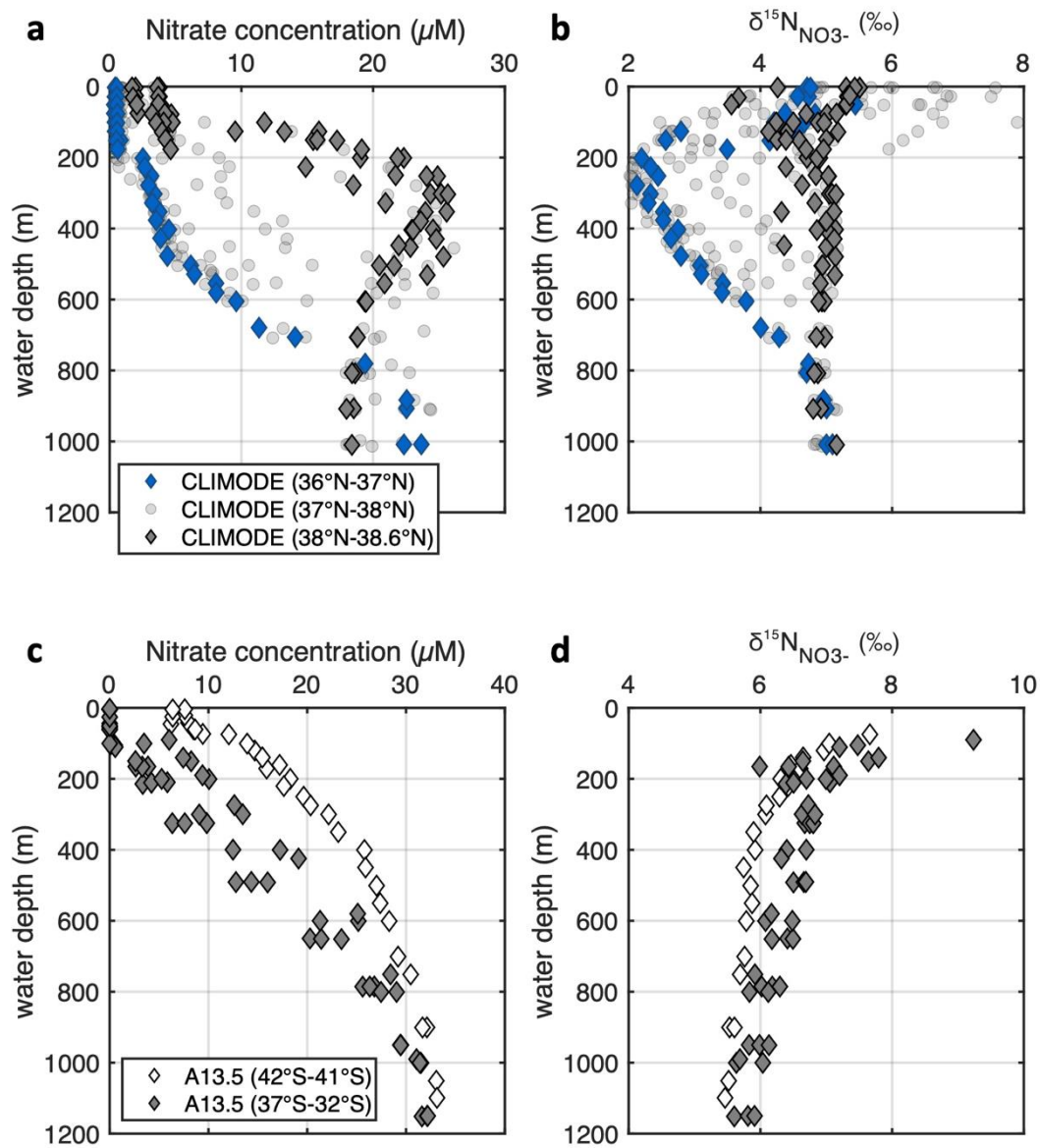


Figure S4. Nitrate concentration and nitrate $\delta^{15}\text{N}$ depth profiles. (a) Nitrate concentration in μM and (b) and nitrate $\delta^{15}\text{N}$ (‰ vs. air) in CLIMODE stations in the North Atlantic, divided into three groups (36-37°N, 37-38 °N and 38-38.6°N). (c) Nitrate concentration in μM and (d) and nitrate $\delta^{15}\text{N}$ (‰ vs. air) in A13.5 stations in the South Atlantic, divided into two groups (42-41°S and 37-32°S).

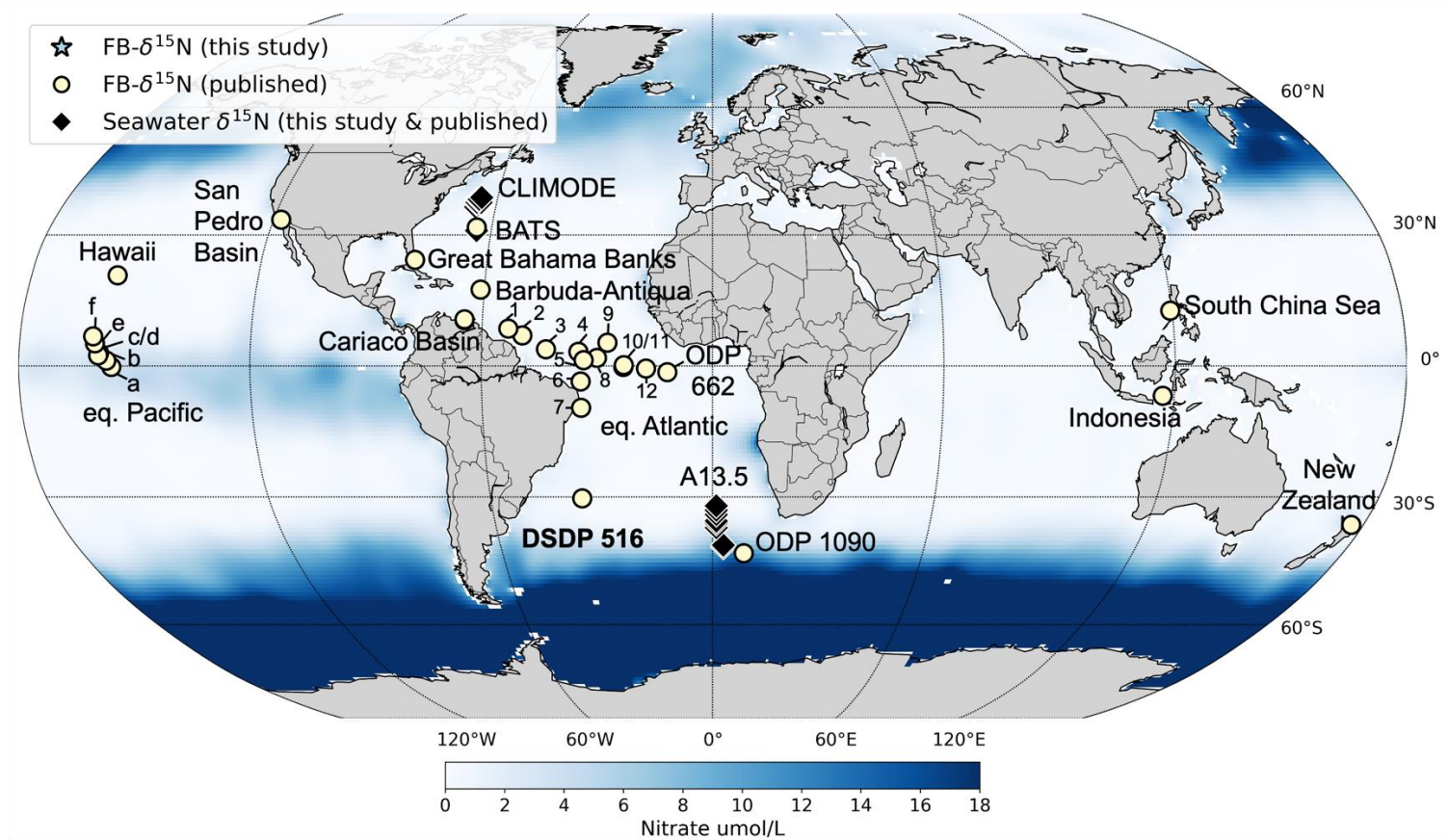


Figure S5. Locations of new (blue star) and published (yellow circles) FB- $\delta^{15}\text{N}$ and seawater $\delta^{15}\text{N}$ data (new and published, black diamonds) used in Figures 5-9. Core locations plotted on mean annual surface nitrate map. Nitrate data from (Garcia et al., 2013) and map generated with Python-based Matplotlib Basemap toolkit (Whitaker and Matplotlib-Team, 2024). Detailed information about core sites, coordinates, analyzed species and references can be found in Table S2.

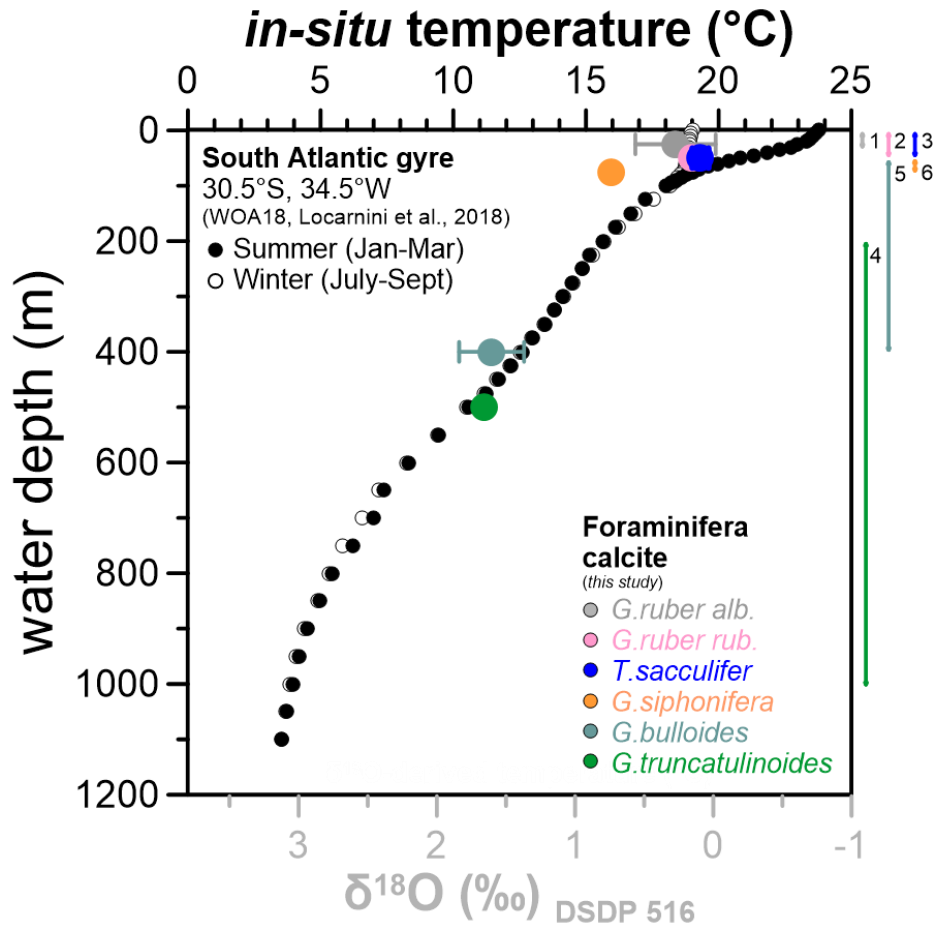


Fig. S6. Temperature depth profile in comparison with oxygen isotopes measured in foraminiferal calcite in DSDP Site 516. Average of Holocene $\delta^{18}\text{O}$ in various foraminifera species in Site 516 (read values from grey x-axis) and $\delta^{18}\text{O}$ -derived temperatures using an online tool (Gaskell and Hull (2022), version 1.2) overlying temperature depth profile approximate depth habitat for each foraminifera species. *In-situ* temperatures in South Atlantic gyre (for winter months (open circles) and summer months (filled circles) (World Ocean Atlas, WOA18, Locarnini et al. (2018)) (read values from black x-axis). Colored bars at the right indicate proposed depth habitats for analysed foraminifera from the literature: ¹ *G. ruber albus* in surface mixed layer (<25m), ² *G. ruber ruber* in surface mixed layer (<50m), ³ *T. sacculifer* in surface mixed layer (<50m), ⁴ *G. truncatulinoides* in thermocline/sub-thermocline, ⁵ *G. bulloides* in surface mixed layer/thermocline (<400 m) and ⁶ *G. siphonifera* in surface mixed layer (50-75m) (Bé et al., 1977; Hemleben et al., 1989).

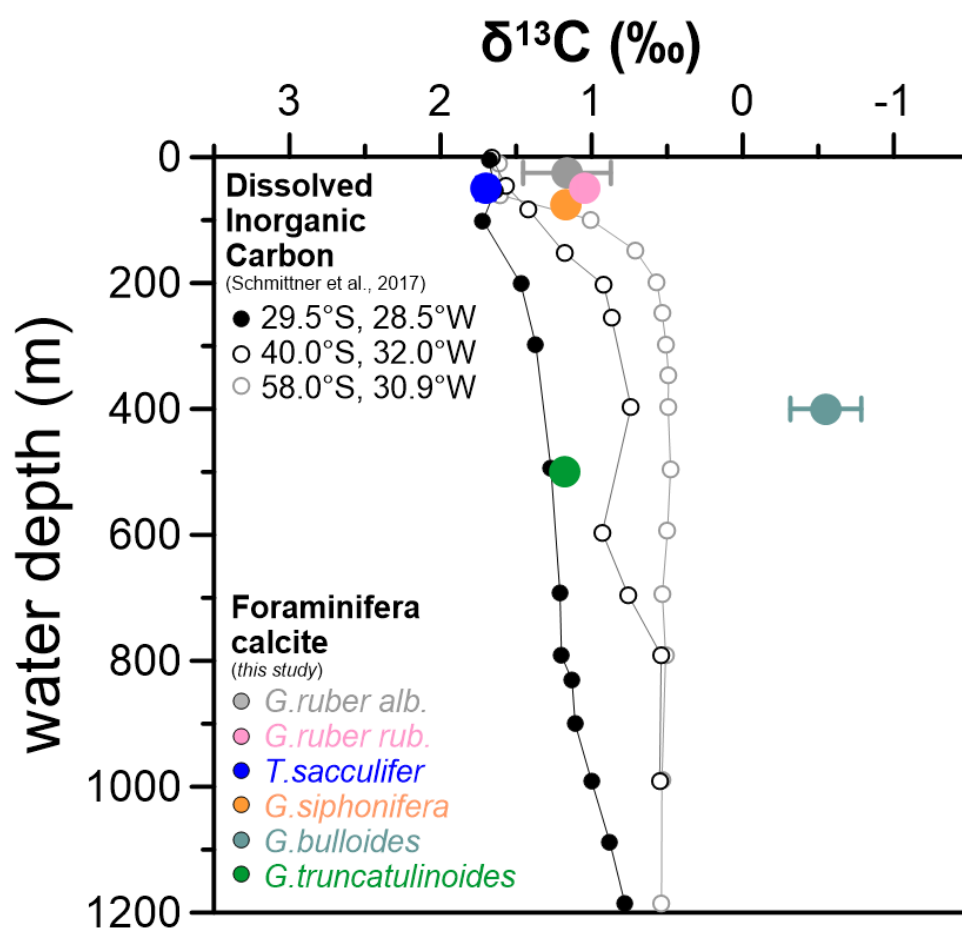


Fig. S7. Dissolved Inorganic Carbon (DIC) carbon isotope depth profile in comparison with carbon isotopes measured on foraminiferal calcite in DSDP Site 516. Average of Holocene $\delta^{13}\text{C}$ measured on species-specific foraminiferal calcite in Site 516. $\delta^{13}\text{C}_{\text{DIC}}$ from South Atlantic stations close to Site 516 (29.5°S, 28.5°W, black) and locations further south (40.0°S, 32.0°W, open black circle and 58.0°S, 30.9°W, open grey circle) (Schmittner et al., 2017).

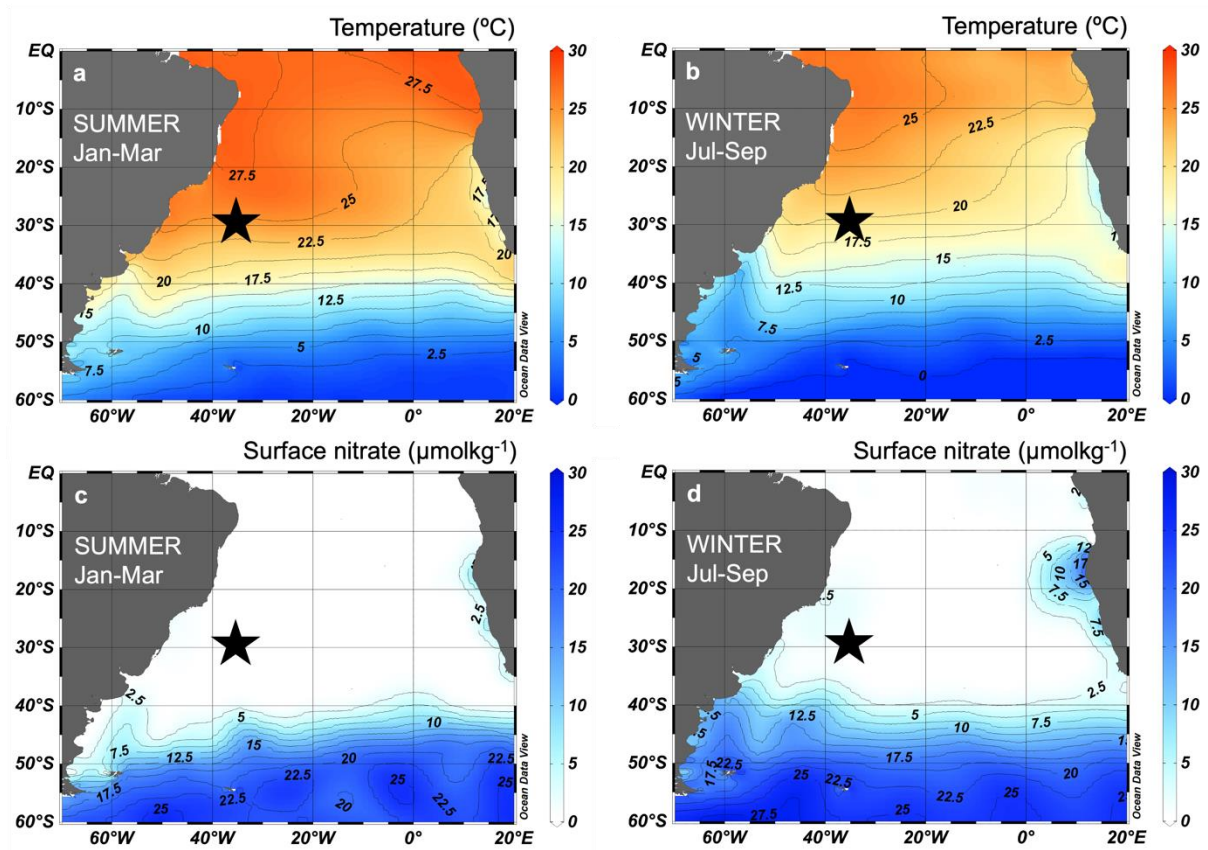


Figure S8. Summer (January to March) and winter (July to September) surface maps for the South Atlantic. (a,b) sea surface temperature (in °C), (c,d) surface nitrate (in $\mu\text{mol/kg}$). Black star indicates location for studied core site DSDP 516. Map generated with Ocean Data View (Schlitzer, 2015) and data set from World Ocean Atlas (Locarnini et al., 2018; Garcia et al., 2013).

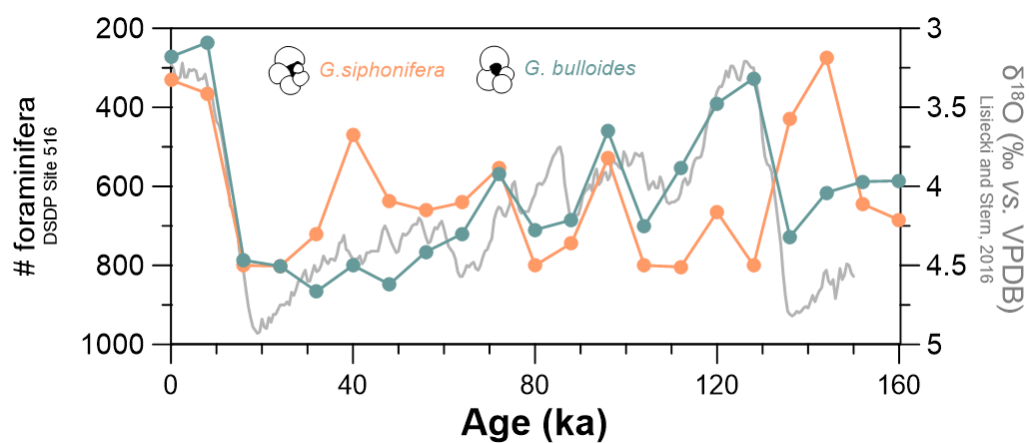


Figure S9. Counted foraminifera specimen per 5cc of sediment in DSDP 516. Orange dots indicate counts for *G. siphonifera*, turquoise dots indicate counts for *G. bulloides* from size fraction 250-400 μm . Note that we stopped counting if number of specimens reached 800 for *G. siphonifera*. Grey line indicates benthic foraminiferal $\delta^{18}\text{O}$ (Lisiecki and Stern, 2016).

References for Supplementary Material:

- Auderset, A., Fripiat, F. o., Creel, R. C., Oesch, L., Studer, A. S., Repschläger, J., Hathorne, E., Vonhof, H., Schiebel, R., and Gordon, L.: Sea Level Modulation of Atlantic Nitrogen Fixation Over Glacial Cycles, *Paleoceanography and Paleoclimatology*, 39, e2024PA004878, <https://doi.org/10.1029/2024PA004878>, 2024.
- Bé, A. W., Hemleben, C., Anderson, O. R., Spindler, M., Hacunda, J., and Tuntivate-Choy, S.: Laboratory and field observations of living planktonic foraminifera, *Micropaleontology*, 155-179, <https://doi.org/10.2307/1485330>, 1977.
- Chappell, J. and Shackleton, N. J.: Oxygen isotopes and sea level, *Nature*, 324, 137-140, <https://doi.org/10.1038/324137a0>, 1986.
- Charles, C. D., Wright, J. D., and Fairbanks, R. G.: Thermodynamic influences on the marine carbon isotope record, *Paleoceanography*, 8, 691-697, <https://doi.org/10.1029/93PA01803>, 1993.
- Costa, K. M., McManus, J. F., Anderson, R. F., Ren, H., Sigman, D. M., Winckler, G., Fleisher, M. Q., Marcantonio, F., and Ravelo, A. C.: No iron fertilization in the equatorial Pacific Ocean during the last ice age, *Nature*, 529, 519-522, <https://doi.org/10.1038/nature16453>, 2016.
- Deuser, W. and Ross, E.: Seasonally abundant planktonic foraminifera of the Sargasso Sea; succession, deep-water fluxes, isotopic compositions, and paleoceanographic implications, *The Journal of Foraminiferal Research*, 19, 268-293, <https://doi.org/10.2113/gsjfr.19.4.268>, 1989.
- Fawcett, S. E., Ward, B. B., Lomas, M. W., and Sigman, D. M.: Vertical decoupling of nitrate assimilation and nitrification in the Sargasso Sea, *Deep Sea Research Part I: Oceanographic Research Papers*, 103, 64-72, <https://doi.org/10.1016/j.dsr.2015.05.004>, 2015.
- Garcia, H. E., Locarnini, R. A., Boyer, T. P., Antonov, J. I., Baranova, O. K., Zweng, M. M., Reagan, J. R., Johnson, D. R., Mishonov, A. V., and Levitus, S.: World ocean atlas 2013. Volume 4, Dissolved inorganic nutrients (phosphate, nitrate, silicate), 2013.
- Gaskell, D. E. and Hull, P. M.: A new online tool for $\delta^{18}\text{O}$ -temperature conversions, *Climate of the Past*, 2022, 1-11, <https://doi.org/10.5194/cp-19-1265-2023>, 2022.
- Gruber, N., Keeling, C. D., Bacastow, R. B., Guenther, P. R., Lueker, T. J., Wahlen, M., Meijer, H. A., Mook, W. G., and Stocker, T. F.: Spatiotemporal patterns of carbon-13 in the global surface oceans and the oceanic Suess effect, *Global biogeochemical cycles*, 13, 307-335, <https://doi.org/10.1029/1999GB900019>, 1999.
- Hemleben, C., Spindler, M., and Anderson, O. R.: Modern planktonic foraminifera, Springer Science & Business Media 1989.
- Knapp, A. N., Sigman, D. M., and Lipschultz, F.: N isotopic composition of dissolved organic nitrogen and nitrate at the Bermuda Atlantic Time-series Study site, *Global Biogeochemical Cycles*, 19, <https://doi.org/10.1029/2004GB002320>, 2005.
- Lessa, D., Morard, R., Jonkers, L., Venancio, I. M., Reuter, R., Baumeister, A., Albuquerque, A. L., and Kucera, M.: Distribution of planktonic foraminifera in the subtropical South Atlantic: depth hierarchy of controlling factors, *Biogeosciences*, 17, 4313-4342, <https://doi.org/10.5194/bg-17-4313-2020>, 2020.
- Lisiecki, L. E. and Stern, J. V.: Regional and global benthic $\delta^{18}\text{O}$ stacks for the last glacial cycle, *Paleoceanography*, 31, 1368-1394, 2016.
- Locarnini, M., Mishonov, A., Baranova, O., Boyer, T., Zweng, M., Garcia, H., Seidov, D., Weathers, K., Paver, C., and Smolyar, I.: World ocean atlas 2018, volume 1: Temperature, 2018.
- Martínez-García, A., Sigman, D. M., Ren, H., Anderson, R. F., Straub, M., Hodell, D. A., Jaccard, S. L., Eglinton, T. I., and Haug, G. H.: Iron fertilization of the Subantarctic Ocean during the last ice age, *Science*, 343, 1347-1350, <https://doi.org/10.1126/science.1246848>, 2014.
- Maslin, M., Shackleton, N., and Pflaumann, U.: Surface water temperature, salinity, and density changes in the northeast Atlantic during the last 45,000 years: Heinrich events, deep water formation, and climatic rebounds, *Paleoceanography*, 10, 527-544, <https://doi.org/10.1029/94PA03040>, 1995.
- Mulitza, S., Dürkoop, A., Hale, W., Wefer, G., and Stefan Niebler, H.: Planktonic foraminifera as recorders of past surface-water stratification, *Geology*, 25, 335-338, [https://doi.org/10.1130/0091-7613\(1997\)025<0335:PFAROP>2.3.CO;2](https://doi.org/10.1130/0091-7613(1997)025<0335:PFAROP>2.3.CO;2), 1997.
- Mulitza, S., Donner, B., Fischer, G., Paul, A., Pätzold, J., Rühlemann, C., and Segl, M.: The South Atlantic oxygen isotope record of planktic foraminifera, *The South Atlantic in the Late Quaternary*, 121-142, https://doi.org/10.1007/978-3-642-18917-3_7, 2003.
- Rashid, H. and Boyle, E. A.: Mixed-layer deepening during Heinrich events: A multi-planktonic foraminiferal $\delta^{18}\text{O}$ approach, *Science*, 318, 439-441, <https://doi.org/10.1126/science.1146138>, 2007.

- Rebotim, A., Voelker, A. H. L., Jonkers, L., Waniek, J. J., Meggers, H., Schiebel, R., Fraile, I., Schulz, M., and Kucera, M.: Factors controlling the depth habitat of planktonic foraminifera in the subtropical eastern North Atlantic, *Biogeosciences*, 14, 827-859, <https://doi.org/10.5194/bg-14-827-2017>, 2017.
- Ren, H., Sigman, D. M., Thunell, R. C., and Prokopenko, M. G.: Nitrogen isotopic composition of planktonic foraminifera from the modern ocean and recent sediments, *Limnology and Oceanography*, 57, 1011-1024, /10.4319/lo.2012.57.4.1011, 2012.
- Rohling, E. J.: Paleosalinity: confidence limits and future applications, *Marine Geology*, 163, 1-11, [https://doi.org/10.1016/S0025-3227\(99\)00097-3](https://doi.org/10.1016/S0025-3227(99)00097-3), 2000.
- Salmon, K., Anand, P., Sexton, P., and Conte, M.: Upper ocean mixing controls the seasonality of planktonic foraminifer fluxes and associated strength of the carbonate pump in the oligotrophic North Atlantic, *Biogeosciences*, 12, 223-235, <https://doi.org/10.5194/bg-12-223-2015>, 2015.
- Schiebel, R.: Planktic foraminiferal sedimentation and the marine calcite budget, *Global Biogeochemical Cycles*, 16, 1065, <https://doi.org/10.1029/2001GB001459>, 2002.
- Schiebel, R. and Hemleben, C.: Modern planktic foraminifera, *Paläontologische Zeitschrift*, 79, 135-148, <https://doi.org/10.1007/BF03021758>, 2005.
- Schiebel, R. and Hemleben, C.: Planktic foraminifers in the modern ocean, Springer, <https://doi.org/10.1007/978-3-662-50297-6>, 2017.
- Schiebel, R., Smart, S. M., Jentzen, A., Jonkers, L., Morard, R., Meilland, J., Michel, E., Coxall, H. K., Hull, P. M., and de Garidel-Thoron, T.: Advances in planktonic foraminifer research: New perspectives for paleoceanography, *Revue de Micropaleontologie*, 61, 113-138, <https://doi.org/10.1016/j.revmic.2018.10.001>, 2018.
- Schlitzer, R.: Data analysis and visualization with Ocean Data View, *CMOS Bulletin SCMO*, 43, 9-13, 2015.
- Schmidt, G. A. and Mulitza, S.: Global calibration of ecological models for planktic foraminifera from core-top carbonate oxygen-18, *Marine Micropaleontology*, 44, 125-140, [https://doi.org/10.1016/S0377-8398\(01\)00041-X](https://doi.org/10.1016/S0377-8398(01)00041-X), 2002.
- Schmittner, A., Bostock, H. C., Cartapanis, O., Curry, W. B., Filipsson, H. L., Galbraith, E. D., Gottschalk, J., Herguera, J. C., Hoogakker, B., and Jaccard, S. L.: Calibration of the carbon isotope composition ($\delta^{13}\text{C}$) of benthic foraminifera, *Paleoceanography*, 32, 512-530, <https://doi.org/10.1002/2016PA003072>, 2017.
- Shackleton, N.: Attainment of isotopic equilibrium between ocean water and the benthonic foraminifera genus *Uvigerina*: isotopic changes in the ocean during the last glacial, 1974.
- Shackleton, N.: Oxygen isotopes, ice volume and sea level, *Quaternary Science Reviews*, 6, 183-190, [https://doi.org/10.1016/0277-3791\(87\)90003-5](https://doi.org/10.1016/0277-3791(87)90003-5), 1987.
- Smart, S. M., Ren, H., Fawcett, S. E., Schiebel, R., Conte, M., Rafter, P. A., Ellis, K. K., Weigand, M. A., Oleynik, S., Haug, G. H., and Sigman, D. M.: Ground-truthing the planktic foraminifer-bound nitrogen isotope paleo-proxy in the Sargasso Sea, *Geochim Cosmochim Acta*, 235, 463-482, <https://doi.org/10.1016/j.gca.2018.05.023>, 2018.
- Tedesco, K., Thunell, R., Astor, Y., and Muller-Karger, F.: The oxygen isotope composition of planktonic foraminifera from the Cariaco Basin, Venezuela: Seasonal and interannual variations, *Marine Micropaleontology*, 62, 180-193, <https://doi.org/10.1016/j.marmicro.2006.08.002>, 2007.
- Thunell, R. and Sautter, L. R.: Planktonic foraminiferal faunal and stable isotopic indices of upwelling: a sediment trap study in the San Pedro Basin, Southern California Bight, Geological Society, London, Special Publications, 64, 77-91, <https://doi.org/10.1144/GSL.SP.1992.064.01.05>, 1992.
- Tolderlund, D. S. and Bé, A. W.: Seasonal distribution of planktonic foraminifera in the western North Atlantic, *Micropaleontology*, 297-329, <https://doi.org/10.2307/1485143>, 1971.
- Whitaker, J. and Matplotlib-team, T.: Basemap 1.4.1 documentation, 2024.